Chapter 7

# Using the Monoplotting Technique for Documenting and Analyzing Natural Hazard Events

Conedera Marco, Bozzini Claudio, Ryter Ueli, Bertschinger Thalia and Krebs Patrik

Additional information is available at the end of the chapter

http://dx.doi.org/10.5772/intechopen.77321

**Abstract**

Historical or present-day oblique terrestrial photographs documenting natural disasters are abundant in archives and may be easily taken nowadays. While in most cases they provide highly informative details, they can hardly be georeferenced, which prevents their systematic use for analyzing and documenting the events and any related signs of damage. In this chapter, we present a monoplotting software program developed at WSL (the WSL Monoplotting Tool) that allows the georeferencing of ordinary individual photographs in order to produce georeferenced vector data by drawing them directly on the photographs and exchanging them with traditional geographic information systems (GIS-Systems). We report on the application of the monoplotting tool on selected study cases of natural events or protection infrastructures in Switzerland.

**Keywords:** event documentation, avalanches, debris flow, landslides, terrestrial pictures, georeferencing, GIS

## 1. Introduction: Documenting natural hazards

Natural events such as avalanches, landslides, rockfall, debris flows, and floods are intrinsic to mountain regions. They become hazards when they impact infrastructures and human beings [1]. Increases in settlement and industrial areas, as well as the ever-increasing need for technology and mobility, make modern society highly vulnerable to natural events, and the resulting potential damage is correspondingly significant [2–5]. In addition, extreme natural events and related impacts are expected to further increase in future due to the ongoing climate change [6–10]. This makes managing natural hazards and mitigating their impact a prerequisite for keeping mountainous areas suitable for inhabitation [11, 12].

Learning from past events represents a very efficient way to expand our knowledge and improve the institutional infrastructure for tackling natural hazards in a sustainable manner [4, 12–14]. This also includes the systematic recording, documentation, and post-processing of ongoing or past events [10, 15].

Based on these considerations, many initiatives have been generated in recent decades for developing methods and protocols for the comprehensive and professional documentation of natural hazards and their marks (see, for instance, the international initiative documentation of mountain disasters (DOMODIS) [16] or the Interreg-Project DIS-ALP—Disaster and Information Systems of Alpine Regions [17]). When trying to build such a systematic register, many difficulties, and bottlenecks may arise concerning both ongoing and past events.

In the case of current disaster events, priority must be given to people rescue and the reestablishment of possibly damaged communication and traffic connections. During such actions, the signs of significant damage may be erased precluding the possibility of subsequent and detailed collection of information documenting the event. Similarly, when there are many simultaneous small events or when events occur in remote and poorly accessible areas and no special devices such as small aerial drones (micro-unmanned aerial vehicles [UAVs]) are available [18, 19], only terrestrial pictures or aerial oblique pictures taken by rescue or technical teams may be available. Nowadays, they are easy to shoot and fairly good in terms of quality even when using portable phones.

Significant past disastrous events dating back to before the first half of the twentieth century are often documented through very detailed terrestrial photographs. They are, however, not georeferenced, and as a result, are not readily suitable for reconstructing the precise location of the event and the damage caused [20, 21]. A great number of historical photographs thus exist that could provide important details on areas under the risk of natural hazards [22, 23].

To make such existing and potential photographic documentation available to extract localized information on natural hazardous events, a user-friendly georeferencing tool for oblique pictures is needed. In this chapter, we report on the main features, needs, and handling of the WSL monoplotting tool (hereafter also referred to as MPT_2.0), a user-friendly software program we developed to orthorectify and georeference oblique pictures, and present some study cases related to past and present natural hazard events in Switzerland.

## 2. What is monophotogrammetry?

Since its appearance in the first half of the nineteenth century and until to the introduction of stereo pairs photography basically consisted of single oblique pictures. Most were produced on glass plates, films or other large-format capture mediums, making it possible to depict, and document detailed landscape features at very high resolutions and quality. Besides providing detailed views of historical landscapes, such single terrestrial photographs have the

http://dx.doi.org/10.5772/intechopen.77321

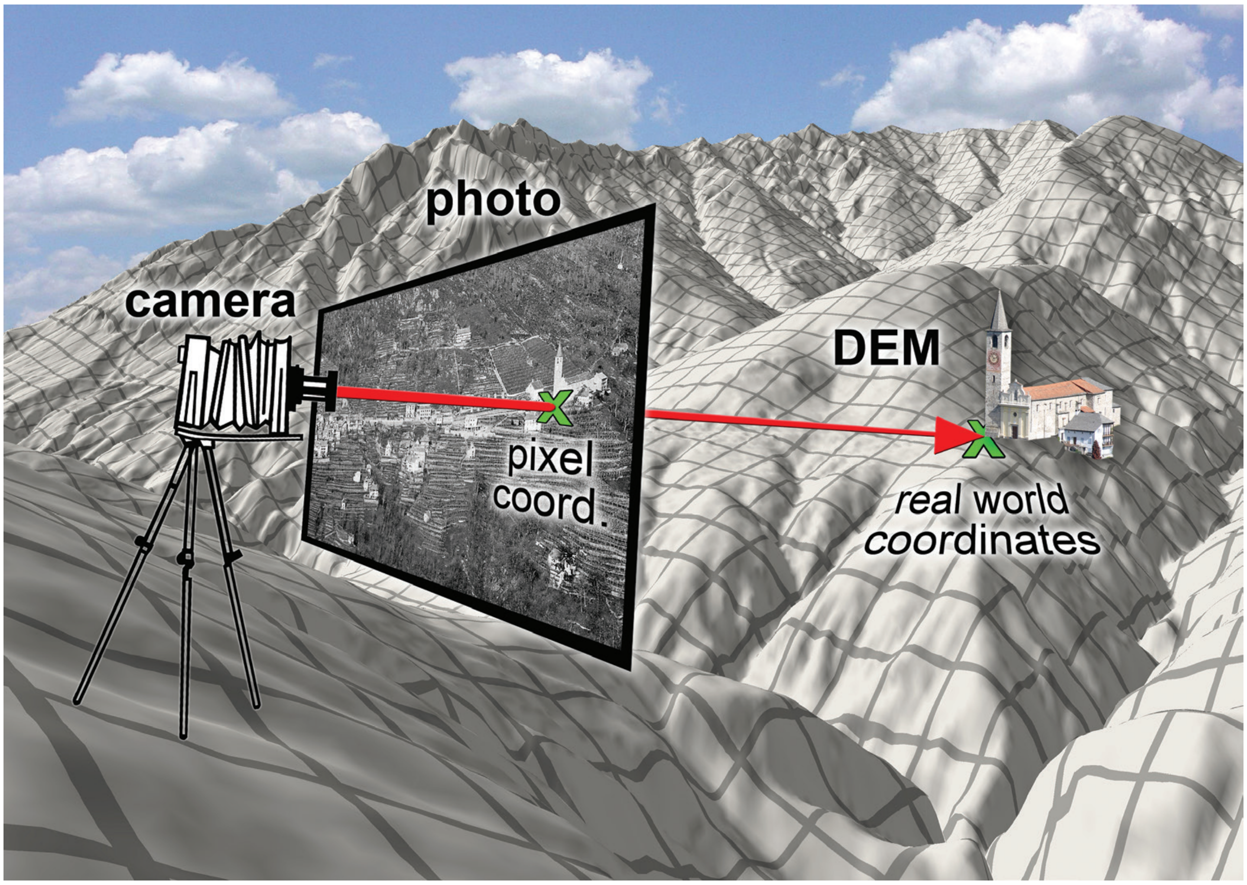


**Figure 1.** Main elements of the monoplotting system: Camera, image, and digital elevation model (DEM).

additional advantage of ease of interpretation as they represent people's everyday perception of the landscape [24]. Accurate georeferencing of such oblique pictures is, however, very difficult. This difficulty has so far prevented reliable quantitative geographical information from being obtained from such photographs.

To overcome this problem, the mono-photogrammetry or monoplotting idea was proposed in the early 1970s [25] wherein a photogrammetric system relates single unrectified, oblique terrestrial, or aerial images to a digital elevation model (DEM) of the corresponding landscape. As visualized in **Figure 1**, the basic idea is to relate to each other camera, picture, and DEM so that a ray from the camera center and going through a selected point in the picture will intersect the terrain DEM at the corresponding landscape point. Such a monoplotting system consists of the following main elements and input data:

- **One or more digital images** shot by digital cameras or resulting from the scanning of historical photographs (e.g., historic pictures on glass plates, postcards). Although the monoplotting system can handle any type of camera and lens (e.g., non-metric cameras), final system accuracy may be heavily influenced by their characteristics.
- **The digital elevation model (DEM),** which is usually structured as a regular data grid (e.g., geotiff raster data). The DEM may refer to the bare ground surface (i.e., Digital Terrain

Model: DTM) or may include vegetation, buildings, and other vertical objects (Digital Surface Model: DSM).

- **Control points (CPs)**, which are precisely and unambiguously identifiable locations (e.g., road and footpath intersections, rocky outcrops, and building corners) on both the image (pixel coordinates) and the landscape (real world coordinates, i.e., latitude, longitude, and altitude of the real-world coordinates). CPs should be at least four or more in number, preferably placed on the ground DTM, and possibly homogeneously distributed over the entire image. The corresponding real-world coordinates may be derived from georeferenced geographical information (e.g., orthophotos, maps, cadaster, DTM, and DSM) or can be directly surveyed in the field instrumentally (e.g., GPS).

Once calibrated in such a monoplotting system, single oblique pictures can also be interpreted three-dimensionally (3D). The main limitation of the monoplotting system is the fact that in mono-photogrammetry, only points on the terrain (DEM-surface) can be precisely located whereas stereo-photogrammetry enables the calculation of the position of any common pixel in the stereo pair.

## 3. The WSL monoplotting tool

The implementation of the monoplotting principle in a practical tool has been restricted by the lack of basic data (i.e., detailed digital elevation models [26]) or the inadequacy of the available computing power [27]. As a result, the pioneering work of Makarovič [25, 28] has long remained isolated. Only in the last 20 years have new software and tools been developed based on the monoplotting principle [29–32]. None of these products, however, really meet the needs of potential end users in terms of operational flexibility and user-friendliness, thus, greatly inhibiting their broad use.

Recently, improvements in digital photography (e.g., high-resolution digital cameras, digitalization of historical pictures in high-resolution) and advancements in computing science have opened new possibilities for developing a specific monoplotting tool with an interface that makes it easy to handle not only by specialized researchers, but also non-expert users for operational purposes [21]. To that end, we developed the WSL monoplotting tool (available at present in the 2.0 version) [24], which has the following main features and characteristics (see also https://www.wsl.ch/monoplotting for detail):

- A user-friendly, intuitive, and self-explanatory interface enabling the simultaneous visualization of one or more photographs of the target landscape as well as of related orthophotos, maps, or other georeferenced representation of the terrain surface (**Figure 2**).
- A computer-assisted, semiautomatic, and interactive calibration process for the camera, including the reconstruction of all elements in the monoplotting system (e.g., snapshot location).
- An immediate estimate of the error for each control point used for the calibration of the oblique photograph.

http://dx.doi.org/10.5772/intechopen.77321

- A simple editor for defining and measuring features of particular interest (e.g., polygons, lines, points, and heights) on the photographs.
- The ability to handle native ERSI-shapefiles.
- Export–import routines allowing data exchange (e.g., CSV or shapefiles) between and from conventional geographic information systems (GIS).

The heart of the tool is the iterative process whereby camera calibration is achieved. This is done in order to precisely estimate and simulate the three intrinsic and the six extrinsic camera parameters. The three intrinsic parameters are the two-pixel coordinates (xc, yc) of the principal point (i.e., the image center), and the principal distance (perpendicular distance from the image to the projection center). The six extrinsic parameters are the three real-word coordinates of the lens pinhole and the three Euler rotation angles $\alpha$ (pan/z-axis), $\beta$ (tilt/y-axis), and $\gamma$ (roll/x-axis) of the camera (see [24, 33] for more details). The calibration routine generates a sequence of collinearity equations commonly used in photogrammetry [34] that estimates and approximates the unknown camera parameters [35] in order to progressively minimize the error of the camera model when applied to the input data. Once camera calibration is achieved, the tool implements a model of all the extrinsic and intrinsic camera parameters, which simulates the original camera setup when the picture was taken. The tool also

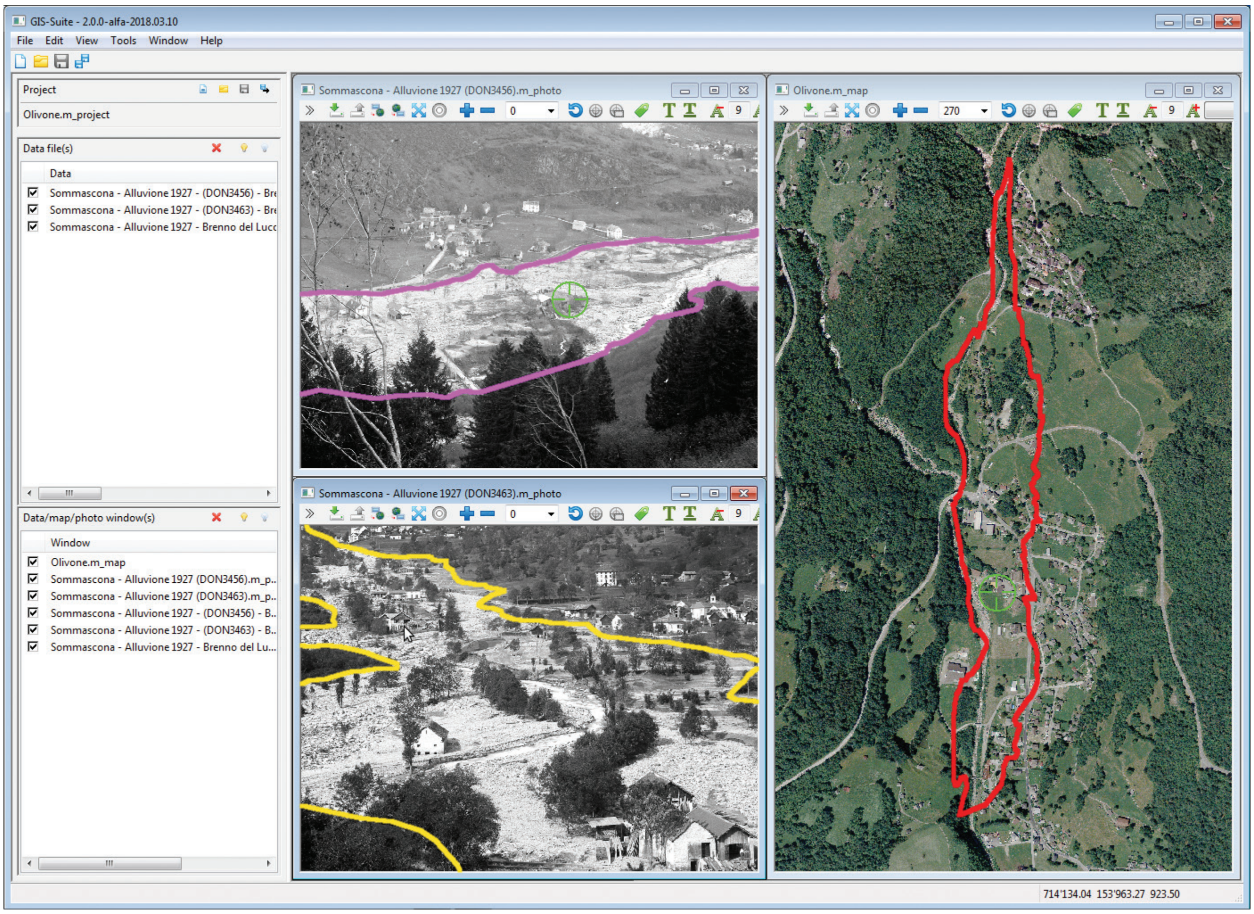


**Figure 2.** The MPT_2.0 applied to the Sommascona flood event (see Example 2). A major strength of the 2.0 release is the option of opening and processing more oblique images or maps of the same area to obtain a complete view of the event.

returns the theoretical 3D errors, which correspond to the deviation between the real-world coordinates of each control point and the corresponding coordinates as calculated from the calibration procedure of the monoplotting system.

It is important to note that shooting point reconstruction is implemented so as to optimize the overlap of the corresponding CPs in the image to be georeferenced and in the georeferenced map, respectively. Thus, the reconstructed theoretical shooting point may not necessarily correspond precisely to the real camera position, and the two may differ by a few centimeters to several meters.

## 4. Applications of the monoplotting tool

We present here selected examples of MPT applications in the field of natural hazards spanning from the reconstruction of historical and current damaging events to the verification of the efficiency of existent infrastructures as well as the related achieved precision and required workload.

### 4.1. Reconstructing historical natural events

A detailed reconstruction of past hazardous events may be of paramount importance for understanding related natural processes, defining danger zones, and planning protection infrastructures. Processing and evaluating pictures of past disastrous events by means of monoplotting is a highly efficient way of retrieving information contained in historical pictures, and transferring it to modern tools such as GIS.

#### *4.1.1. Example 1: the Sasso Rosso slope failure: 1898, Airolo*

The Sasso Rosso area above the village of Airolo (Canton of Ticino) turned into an unstable slope due to the decompression caused by post-glacial ice retreat. Local authorities were aware of this and put the area under surveillance. Initial significant slope movement began in the summer of 1898, followed by three slides of increasing size in December of the same year. Fortunately, the authorities decided at that time to close the school and evacuate the endangered part of the village. Just before midnight in the night of the December 27, 1898, a series of slides occurred, with a volume totaling 500,000 $m^3$, reaching part of the village and destroying a hotel, 11 houses, and 15 stables, while causing three deaths.

According to the reconstructed and digitalized perimeter of the debris deposit as reported in **Figure 3**, the area in question covered ca. 425,000 $m^2$. The MPT_2.0 also enables the projection of the digitalized deposit perimeter on a historical picture prior to the debris flow (**Figure 4**), clearly identifying the area and the buildings destroyed by the event.

#### *4.1.2. Example 2: flood in Sommascona: 1927, Olivone*

During the autumn of 1927, southern Switzerland and northern Italy experienced a period of heavy precipitation that caused several flood events of varying severity. The worst occurred

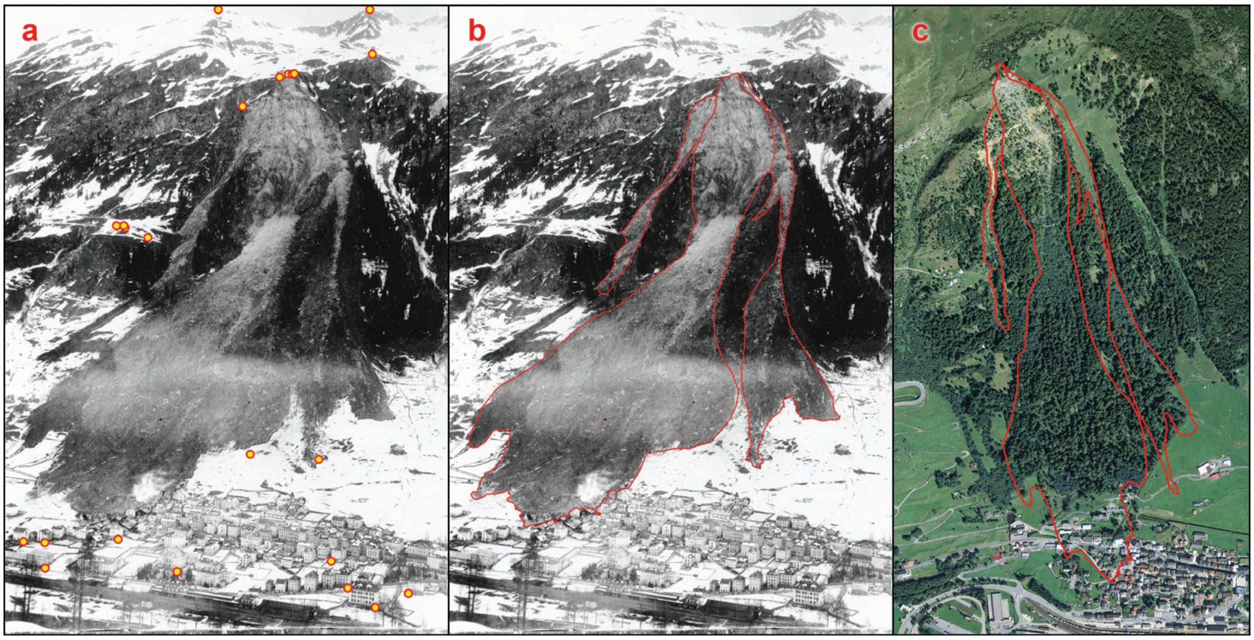


**Figure 3.** The Sasso Rosso slope failure (Airolo, 1898). (a) Original obliques images with control points. (b) Digitalization of the slide contour on the original obliques images. (c) Projection of the slide perimeter on a current orthophoto (modified from Conedera et al. [21]).

**Figure 4.** The Sasso Rosso slope failure (Airolo, 1898). Projection of the slide perimeter on an oblique terrestrial image of the area prior to the event (source: Conedera et al. [21]).

in Ticino (Switzerland) on Sunday afternoon on September 25, 1927, as a consequence of a strong and long-lasting waterspout above the mountain village of Olivone. This flood is still considered to be the most damaging natural event of the last century in the region. It destroyed part of the village of Campo Blenio and flooded the plain of Olivone over an area of at least 199,366 $m^2$ (ArcGIS computation of the perimeter as digitalized with the monoplotting tool), affecting two sawmills and several private buildings (**Figure 5**). Due to the favorable weekday, no fatalities were recorded.

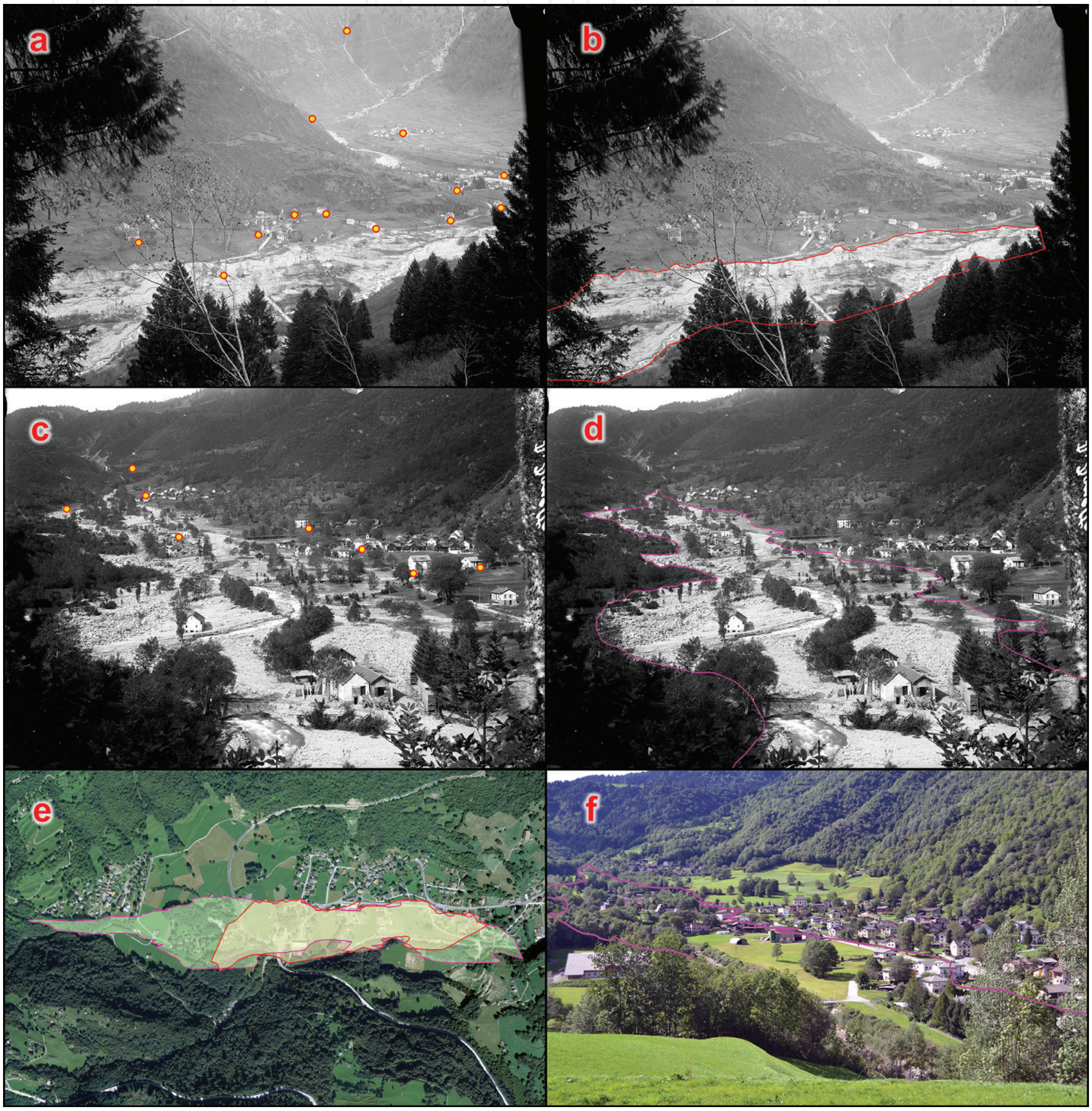


**Figure 5.** Flood of the Sommascona plain (Olivone, 1927). (a + b) original oblique images with control points. (c + d) Digitalization of the flood contours on the original oblique image. (e) Projection of the digitalized flood contours on the current orthophoto. (f) Projection of the digitalized flood contours on the current oblique terrestrial image (modified from Conedera et al. [21]).

### 4.2. Documenting natural events in real time

Real-time documentation of the fresh marks of hazardous events makes it possible to capture many important details that may enable a realistic reconstruction of the processes that occurred. Such improved understanding of underlying processes is, in turn, of paramount importance to improve the simulation and modeling of natural hazards as well as possible prevention and mitigation measures. Thanks to the monoplotting approach actual natural hazards or natural hazard-related situations can be easily processed and mapped, regardless of the remoteness or accessibility of the area in question.

#### *4.2.1. Example 3: avalanches in Hasliberg: 2018, Meiringen*

For safety reasons, the security managers of the Hasliberg ski resort record all artificially provoked and natural occurring avalanches by means of SLF pro tools, which is a map-based information system (https://www.slf.ch/en/services-and-products/protools.html). For this purpose, they roughly estimate the avalanche contour in the field. Over time, a conspicuous number of events have been entered into the system, causing the cantonal forest service to migrate all data into the official historical avalanche cadaster. Before doing this, however, the reliability of the empirical approach used by the security managers required testing. To that end, an aerial recognition mission was organized on January 24, 2018, and a number of fresh avalanches were photographically documented to be processed with the MPT_2.0.

Despite the difficulty in identifying suitable CPs in a snowy landscape, the theoretical 3D-error achieved is more than acceptable (**Table 1**), and each single registered avalanche perimeter could be measured and compared with the estimated contours by the ski resort managers. The comparison revealed significant differences with a trend toward overestimating the avalanche size by the local ski managers (**Figure 6**). Single events should thus be verified by the mean of the MPT_2.0 before their migration into the official historical avalanche cadaster.

#### *4.2.2. Example 4: Spitzhorn rockslide: 2017, Gstaad*

In October 2017, a rockslide moved a volume of ca. 50,000 m$^3$ downhill from the west slope of the Spitzhorn mountain. The event took place in a single main slide preceded by individual

| Study case | | Object | Image quality | Control points | Theoretical 3D-error (m) | | |
|---|---|---|---|---|---|---|---|
| | | | | | Min | Max | Mean |
| 1. | Airolo | Slope failure | Medium | 20 | 0.2 | 3.0 | 0.9 |
| 2. | Olivone | Flood (a) | Good | 8 | 0.1 | 2.4 | 0.9 |
| | | Flood (b) | Good | 13 | 0.2 | 0.9 | 0.4 |
| 3. | Meiringen | Avalanche | Good | 5 | 0.1 | 0.6 | 0.2 |
| 4. | Gstaad | Rockslide | Good | 6 | 0.1 | 2.3 | 0.5 |
| 5. | Adelboden | Snow bridges | Good | 6 | 0.1 | 1.0 | 0.3 |

**Table 1.** Achieved theoretical 3D-error for the presented study cases.

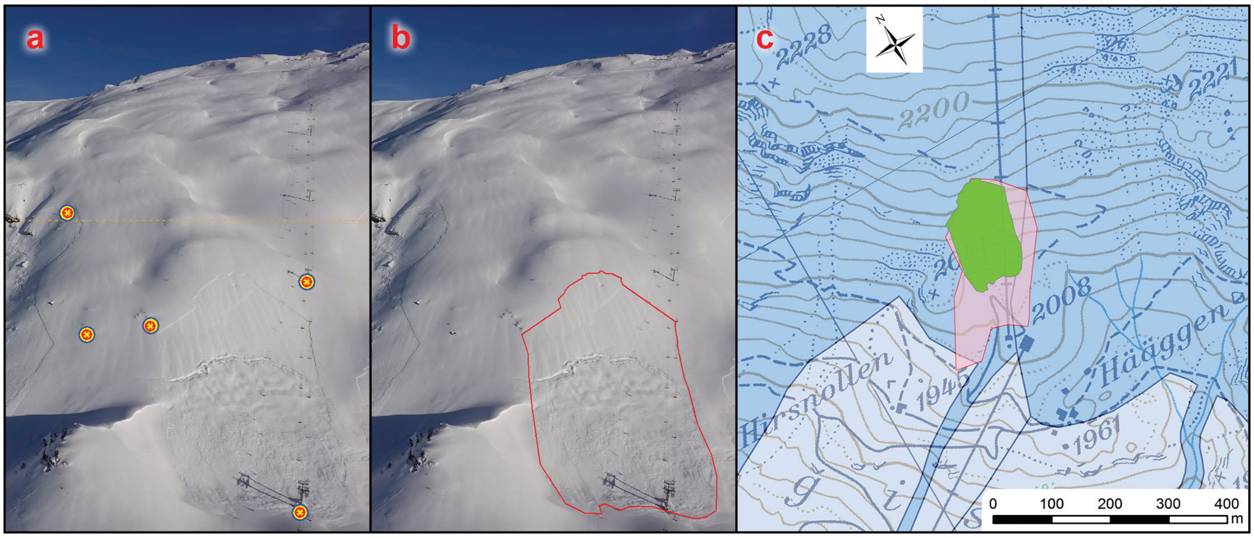


**Figure 6.** Avalanches in the Hasliberg ski area (Meiringen, 2018). (a) Original oblique image with control points. (b) Digitalization of the avalanche perimeter on the original image. (c) Map showing the area in question and avalanches over the years (blue), the avalanche perimeter as estimated by the ski resort managers (red), and as measured by the MPT_2.0 (green).

rockfalls, which gave security managers the opportunity to block all vehicular and pedestrian access, thus preventing fatalities. Nevertheless, the rockslide caused significant damage to the forest, the electric line, and trails.

In order to assess the involved area precisely, we used the MPT_2.0 to process an oblique picture taken during a field inspection. Despite the difficulty in selecting suitable CPs (**Figure 7**), the achieved precision (**Table 1**) and the related time investment (**Table 2**) for analyzing the image are acceptable.

### 4.3. Verifying the efficiency of protection infrastructures

Documenting protection infrastructures during particular events or climatic situations may also be very helpful when assessing their functional capability and reliability in preventing natural events. Our final example relates to the assessment of the dimensioning and efficiency of snow barriers as protection against avalanches under real conditions.

#### *4.3.1. Example 5: analyzing the functionality of snow bridges: 2018, Adelboden*

The functional capability of snow bridges against avalanche detachment highly depends on the correct dimensioning of the supporting structures. A prerequisite for snow bridge efficiency is that the snow never rises above the supporting area of the structure. When these conditions are not satisfied for a significant part of the snow bridge, avalanches can detach from the exceeding snow cover, damaging the snow bridges located downhill, and threatening the infrastructures in the danger zone.

Snow bridge reliability can be best assessed in real conditions during exceptional snow cover conditions. This was the case in Adelboden (Canton Berne, Switzerland) during the heavy snowfalls combined with strong snow blowing winds that repeatedly occurred in the winter

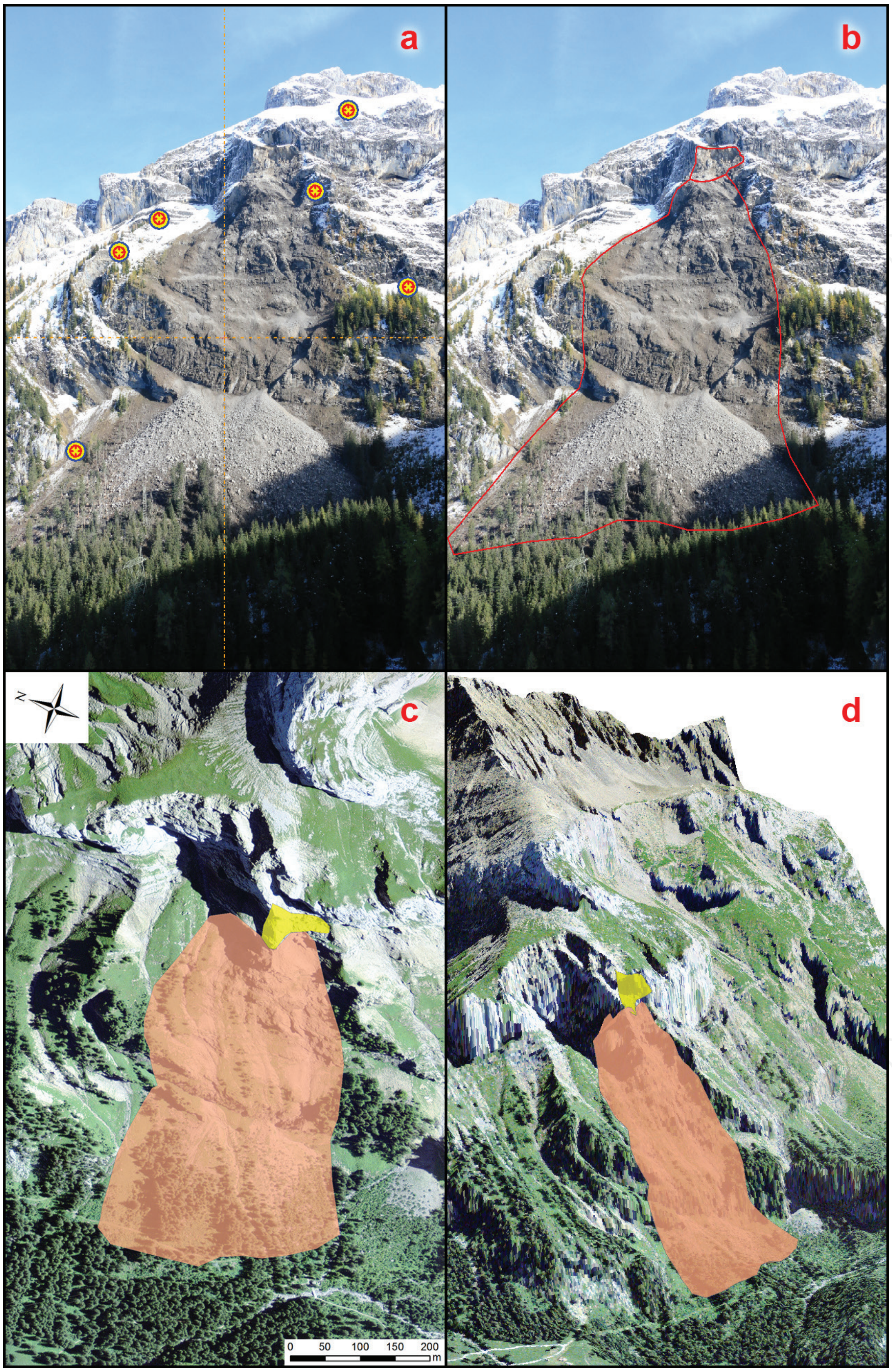


**Figure 7.** Spitzhorn rockslide (Gstaad, 2017). (a) Original oblique images with control points. (b) Digitalization of the detachment and transit/deposit zone on the original oblique image. (c) Projection of the digitalized contours on the current orthophoto. (d) Projection and 3D viewing of the digitalized zones in ESRI ArcScene. Yellow contours = detachment zone; orange contours = transit and deposit zone.

| Working steps | Time investment (min) | | |
|---|---|---|---|
| | Min | Mean | Max |
| Preparation of basic data for the area in question (DEM, maps, orthophotos, images) | 10 | 20 | 30 |
| Choosing and fixing control points (CPs) | 10 | 30 | 90 |
| Camera calibration | 5 | 15 | 30 |
| Digitalizing target objects | 5 | 15 | 20 |
| Import/export | 5 | 5 | 5 |
| Total | 35 | 90 | 175 |

**Table 2.** Average time investment for individual working steps when processing an image with the WSL monoplotting tool.


**Figure 8.** Snow bridges (Adelboden, 2018). (a) Original oblique image of the snow bridge constructions with control points. (b) Digitalization of the snow bridges. (c) Projection of the digitalized bridges on the current orthophoto highlighting in blue the parts covered by snow.

season of 2017/2018, which caused a partial blanketing of the snow bridges in the upper part of the area in question. On January 24, 2018, which was 2 days after the end of a heavy snowfall event, a helicopter recognition mission was organized and the snow bridge area was photographed in order to document the blanketed parts (**Figure 8a**).

Through the georeferencing process of the MPT_2.0 (**Figure 8b**), the bridges were digitalized and exported to a GIS file, making it possible to identify the blanketed snow bridge parts, which may fail in their protection function (**Figure 8c**).

## 5. Discussion

The MPT_2.0 has proven to be a highly suitable instrument for georeferencing and documenting the impact of geophysical (landslides, avalanches) and hydrological (debris flows, floods) natural hazards. As reported in **Table 1**, the achieved theoretical precision for the presented study cases ranges from decimeters to a few meters, which is more than acceptable for practical purposes. In addition to the image quality and its resolution in particular, the precision of the system additionally depends on the DEM resolution and on the number, clarity, and distribution of the control points. The combination of highly resolved DEM and unambiguous (e.g., constructions), well-distributed CPs easily result in sub-metric precision.

Local significant deviations in the reconstructed position in monoplotting with respect to the real world may, in contrast, occur when there are objects in the background landscape of an image, or when areas in the landscape display a small incidence angle with respect to the camera ray. Here, small imprecisions in clicking on the corresponding image pixel may result in a great displacement of the corresponding real point where the ray intersects the DEM. In case of crests and ridges, the ray may even overshoot the DEM and hit the background landscape or get lost in the sky.

Additional sources of error are changes in the terrain morphology that took place between the time the image was shot and the DEM measurement. These may have originated in anthropogenic mass movements or by natural events such as landslides. In the latter case, only the untouched margins of the terrain changes may be localized with the monoplotting technique (see **Figure 4**).

Similar achievement potential and limitations of the MPT_2.0 in terms of usefulness and achievable precision have been reported in independent scientific studies in the field of historical landscape reconstructions [36] and treeline ecotone dynamics [37].

According to our accumulated experience utilizing the MPT_2.0, the required time investment highly depends on (a) the epoch of the event (the further back in time, the more the landscape may have changed, and the fewer available control points), (b) the quality of the image regarding the extent and form of the object to be digitalized (from local land slide to regional floods), and (c) on the available information (shooting location in particular). Thus far, most oblique images with suitable CPs were successfully processed with the MPT_2.0 in a short time. The most time-consuming steps relate to the preparation of basic information such as the DEM, maps, orthophotos, images of the area in question, and the definition of the CPs (**Table 2**).

## 6. Conclusions

The main aim of using the WSL monoplotting tool (MPT_2.0) is to document in real time and reconstruct the effects of natural events before damage and signs in the landscape are removed or disappear. In this respect, the tool was found to be very flexible, enabling the operator to combine images from different epochs, and points of view that describe the same event. The possibility of georeferencing such images by reconstructing the unknown shooting point enables the use of oblique aerial photographs taken from helicopters, which in turn, opens the door to documenting natural events in highly inaccessible sites (see Example 5, blanketed snow bridges).

When suitable photographic material exists, even events dating back more than a century can be reconstructed with very satisfactory precision (see Example 1, Sasso Rosso area, Airolo). Similarly, also the extent and the severity of past pest attacks, diseases or wildfires can be retrospectively reconstructed provided, there is a suitable photographic documentation. The MPT_2.0 could also be very useful in combination with the surveillance system cameras for automatic wildfire detection. When oblique images of the landscape from such fixed cameras are georeferenced in the monoplotting system, the pixel coordinates of the fire detection can also be immediately expressed in real-world coordinates (including the possible error) when a fire ignition spot is detected.

In contrast, less practicable is the use of the MPT_2.0 for the real-time documentation of dynamic processes such as the localization of a fire line front in fast spreading, large wildfires. In such cases, unmanned aerial vehicles (UAVs, drones) may be most suitable for producing real-time, georeferenced images of the fire front, or residual burning.

At present, the 2.0 release of the WSL Monoplotting Tool (MPT 2.0) is available at the project site (www.wsl.ch/monoplotting) and freely usable for research purposes. Please refer to this webpage for details on the terms and conditions of use, services, and tutorial options.

## Acknowledgements

**Figure 1** is published with the kind permission of SAGE Publications. Although partially modified, **Figures 3–5** are published with the kind permission of the Swiss Forestry Journal.

## Author details

Conedera Marco[1]*, Bozzini Claudio[1], Ryter Ueli[2], Bertschinger Thalia[2] and Krebs Patrik[1]

*Address all correspondence to: marco.conedera@wsl.ch

1 Swiss Federal Institute for Forest, Snow and Landscape Research (WSL), Insubric Ecosystems Research Group, Cadenazzo, Switzerland

2 Forest Service Canton Berne, Natural Hazards Section, Interlaken, Switzerland

## References

[1] Frey W, Wilhelm C, Gesamtbetrachtung KB N-v E z. Schweizerische Zeitschrift für Forstwesen. 2001;**152**(5):199-203. DOI: 10.3188/szf.2001.0199

[2] Wehrli A, Brang P, Maier B, Duc P, Binder F, Lingua E, Ziegner K, Kleemayr K, Dorren L. Schutzwaldmanagement in den Alpen—eine Übersicht. Schweizerische Zeitschrift für Forstwesen. 2007;**158**(6):142-156. DOI: 10.3188/szf.2007.0142

[3] Hilker N, Badoux A, Hegg C. The Swiss flood and landslide damage database 1972-2007. Natural Hazards and Earth System Sciences. 2009;**9**:913-925. DOI: 10.5194/nhess-9-913-2009

[4] Klinke A, Renn O. Nachhaltiger Umgang mit natürlichen Risiken: antizipativ, integrativ und interdisziplinär. Schweizerische Zeitschrift für Forstwesen. 2011;**162**(12):442-453. DOI: 10.3188/szf.2011.0442

[5] Schwendtner B, Papathoma-Kohle M, Glade T. Risk evolution: How can changes in the built environment influence the potential loss of natural hazards? Natural Hazards and Earth System Sciences. 2013;**13**:2195-2207. DOI: 10.5194/nhess-13-2195-2013

[6] Frei CR, Schöll R, Fukutone S, Schmidli J. Vidale PL future changes of precipitation extremes in Europe. Journal of Geophysical Research. 2006;**111**:D06105. DOI: 10.1029/2005JD005965

[7] Fowler HJ, Ekström M, Blenkinsop S, Smith AP. Estimating change in extreme European precipitation using a multimodel ensemble. Journal of Geophysical Research. 2007;**112**: D18104. DOI: 10.1029/2007JD008619

[8] Beniston M, Stephenson DB, Christensen OB, Ferro CAT, Frei C, Goyette S, Halsnaes K, Holt T, Jylhä K, Koffi B, Palutikof J, Schöll R, Semmler T, Woth K. Future extreme events in European climate: An exploration of regional climate model projections. Climatic Change. 2007;**81**:71-95. DOI: 10.1007/s10584-006-9226-z

[9] Marty C, Phillips M, Lehning M, Wilhelm C, Bauder A. Klimaänderung und Naturgefahren in Graubünden. Schweizerische Zeitschrift für Forstwesen. 2009;**160**(7):201-209. DOI: 10.3188/szf.2009.0201

[10] Papathoma-Köhle M, Promper C, Glade T. A common methodology for risk assessment and mapping of climate change related zazards—Implications for climate change adaptation policies. Climate. 2016;**4**(8):1-23. DOI: 10.3390/cli4010008

[11] Hollenstein K, Hess J. Integrales Management von gravitativen Naturrisiken in der Schweiz. Schweizerische Zeitschrift für Forstwesen. 2011;**162**(12):454-463. DOI: 10.3188/szf.2011.0454

[12] Nquot I, Kulatunga U. Flood mitigation measures in the United Kingdom. In: Proceedings of the 4th International Conference on Building Resilience, Incorporating the 3rd Annual Conference of the Android Disaster Resilience Network, Manchester (United Kingdom). September 8-11, 2014. pp. 81-87

[13] Garcia C, Blahut J, Angignard M, Pasuto A. The importance of the lessons learnt from past disasters for risk assessment. In: VanAsch T, Corominas J, Greiving S, Malet JP, Sterlacchini S, editors. Mountain Risks: From Prediction to Management and Governance. Springer; 2014. pp. 275-284. DOI: 10.1007/978-94-007-6769-0_9

[14] Uhlemann S, Thieken AH, Merz B. A quality assessment framework for natural hazard event documentation: Application to trans-basin flood reports in Germany. Natural Hazards and Earth System Sciences. 2014;**14**:189-208. DOI: 10.5194/nhess-14-189-2014

[15] Adams MS, Fromm R, Lechner V. High-resolution debris flow volume mapping with unmanned aerial systems (UAS) and photogrammetric techniques. July 12-19, 2016. pp. 749-755

[16] Hübl J, Kienholz H, Loipersberger A, editors. DOMODIS. Dokumentation alpiner Naturereignisse. Klagenfurt: Internationale Forschungsgesellschaft Interpraevent; 2006. 44 p. ISBN: 3-901164-07-3

[17] PLANALP (Platform on Natural Hazards of the Alpine Convention). Dokumentation von Naturereignissen—Feldanleitung. Innsbruck/Bern; 2006. 64 p

[18] Giordan D, Manconi A, Remondino F, Nex F. Use of unmanned aerial vehicles in monitoring application and management of natural hazards. Geomatics Natural Hazards & Risk. 2017;**8**:1-4. DOI: 10.1080/19475705.2017.1315619

[19] Huang H, Long J, Yi W, Yi Q, Zhang G, Lei B. A method for using unmanned aerial vehicles for emergency investigation of single geo-hazards and sample applications of this method. Natural Hazards and Earth System Sciences. 2017;**17**:1961-1979. DOI: 10.5194/nhess-17-1961-2017

[20] Copien C, Frank C, Becht M. Natural hazards in the Bavarian alps: A historical approach to risk assessment. Natural Hazards. 2008;**45**:173-181. DOI: 10.1007/s11069-007-9166-6

[21] Conedera M, Bozzini C, Scapozza C, Rè L, Ryter U, Krebs P. Anwendungspotenzial des WSL-Monoplotting-Tools im Naturgefahrenmanagement. Schweizerische Zeitschrift für Forstwesen. 2013;**164**(7):173-180. DOI: 10.3188/szf.2013.0173

[22] Edwards M. The United-States geophysical-data center can provide natural hazards damage photographs. Environmental Geology and Water Sciences. 1991;**18**:81-81. DOI: 10.1007/bf01704660

[23] NGDC (NOAA National Geophysical Data Center). Natural Hazards Image Database [Internet]. 2018. Available from: http://oregonexplorer.info/content/noaa-national-geophysical-data-center-ngdc-natural-hazards-image-database [Accessed: March 20, 2018]

[24] Bozzini C, Conedera M, Krebs P. A new monoplotting tool to extract georeferenced vector data and orthorectified raster data from oblique non-metric photographs. International Journal of Heritage in the Digital Era. 2013;**1**(3):500-518. DOI: 10.1260/2047-4970.1.3.499

[25] Makarovič B. Digital monoplotters. The ITC Journal. 1973;**4**:583-600

[26] Hodgson ME, Bresnahan P. Accuracy of airborne lidar-derived elevation: Empirical assessment and error budget. International Archives for Photogrammetry and Remote Sensing. 2004;**70**(3):331-339. DOI: 10.14358/PERS.70.3.331

[27] Ceruzzi PE. A History of Modern Computing. Cambridge: MIT Press; 2003. 445 p. ISBN: 0-262-53203-4

[28] Makarovič B. Data base updating by digital monoplotting. The ITC Journal. 1982;**4**:384-390

[29] Doytsher Y, Hall JK. FORTRAN programs for coordinate resection using an oblique photograph and high-resolution DTM. Computers & Geosciences. 1995;**21**(7):895-905. DOI: 10.1016/0098-3004(95)00023-2

[30] Aschenwald J, Leichter K, Tasser E, Tappeiner U. Spatio-temporal landscape analysis in mountainous terrain by means of small format photography: A methodological approach. IEEE Transactions on Geoscience and Remote Sensing. 2001;**39**(4):885-893. DOI: 10.1109/36.917917

[31] Corripio JG. Snow surface albedo estimation using terrestrial photography. International Journal of Remote Sensing. 2004;**25**(24):5705-5729. DOI: 10.1080/01431160410001709002

[32] Fluehler M, Niederoest J, Akca D. Development of an educational software system for the digital monoplotting. In: Proceedings of the International Society for Photogrammetry and Remote Sensing, Working group VI/1–VI/2 (Tools And Techniques for E-Learning), Potsdam (Germany). June 1-3, 2005. 6 p

[33] Kraus K. Photogrammetry. Fundamentals and Standard Processes. Vol. 1. Bonn: Dümmlers; 1993. 397 p. ISBN: 13: 9783427786849

[34] Ghosh SK. Fundamentals of Computational Photogrammetry. New Delhi: Concept Publishing Company; 2005. 254 p. ISBN: 13: 9788180691874

[35] Strausz DA. An Application of Photogrammetric Techniques to the Measurement of Historic Photographs. Oregon State University, Department of Geosciences; 2001

[36] Stockdale CA, Bozzini C, Macdonald SE, Higgs E. Extracting ecological information from oblique angle terrestrial landscape photographs: Performance evaluation of the WSL Monoplotting tool. Applied Geography. 2015;**63**:315-325. DOI: 10.1016/j.apgeog.2015.07.012

[37] McCaffrey DR, Hopkinson C. Assessing fractional cover in the alpine treeline ecotone using the WSL Monoplotting tool and airborne Lidar. Canadian Journal of Remote Sensing. 2017;**43**:504-512. DOI: 10.1080/07038992.2017.1384309

IntechOpen